

The Zeeman Effect

Robert DeSerio

Ph 461

Objective: In this experiment, you will measure the small energy shifts in the magnetic sublevels of atoms in “weak” magnetic fields. The visible light from transitions between various multiplets is dispersed in a 1.5 m grating spectrograph and observed with a telescope. Each observed line consists of a group of closely spaced unresolved lines from the emissions among the different magnetic sublevels within each multiplet. Using a polarizer and Fabry-Perot interferometer, ring patterns are observed within each spectrographically resolved line. The patterns are measured as a function of the strength of the magnetic field to determine the g -factor of the multiplet.

1 Theory

1.1 Magnetic moment

The electron (charge $-e$, mass m) has an intrinsic spin angular momentum \mathbf{s} and an intrinsic magnetic moment $\boldsymbol{\mu}_s$ that can be expressed as:

$$\boldsymbol{\mu}_s = -2\frac{\mu_B}{\hbar}\mathbf{s} \quad (1)$$

where $\mu_B = e\hbar/2mc$ is called the Bohr magneton and is effectively the atomic unit of magnetic moment. (The factor 2 in Eqn. 1 is a prediction of Dirac’s relativistic theory of electron spin, and when quantum electrodynamic effects are included increases by about 0.1%)

If a spinless electron is orbiting a nucleus in a state of angular momentum $\boldsymbol{\ell}$, it behaves like a current loop with a magnetic moment $\boldsymbol{\mu}_\ell$ proportional to

ℓ :

$$\boldsymbol{\mu}_\ell = -\frac{\mu_B}{\hbar}\boldsymbol{\ell}, \quad (2)$$

The nucleus also often has a magnetic moment, but because of the large nuclear mass, it is much smaller than that of the electron, and at the resolutions involved in this experiment its effects will be unobservable.

When electron spin and orbital angular momentum are simultaneously taken into account, the magnetic moment of each electron in the atom becomes:

$$\boldsymbol{\mu}_e = -\frac{\mu_B}{\hbar}(2\mathbf{s} + \boldsymbol{\ell}) \quad (3)$$

For an N -electron atom, the total magnetic moment is thus:

$$\boldsymbol{\mu} = \frac{\mu_B}{\hbar} \sum_{i=1}^N -(2\mathbf{s}_i + \boldsymbol{\ell}_i), \quad (4)$$

or

$$\boldsymbol{\mu} = -\frac{\mu_B}{\hbar}(2\mathbf{S} + \mathbf{L}), \quad (5)$$

where $\mathbf{S} = \sum \mathbf{s}_i$ and $\mathbf{L} = \sum \boldsymbol{\ell}_i$. Since $\mathbf{J} = \mathbf{L} + \mathbf{S}$ this is usually written:

$$\boldsymbol{\mu} = -\frac{\mu_B}{\hbar}(\mathbf{J} + \mathbf{S}). \quad (6)$$

1.2 Magnetic energy

The energy V of a magnetic moment $\boldsymbol{\mu}$ in a uniform magnetic field \mathbf{B} depends on the relative angle between them:

$$V = -\boldsymbol{\mu} \cdot \mathbf{B} \quad (7)$$

With the B -field taken along the z -direction (and having a strength B) this becomes:

$$V = -B\mu_z. \quad (8)$$

In the absence of a magnetic field, the unperturbed energy levels of a free atom are always rigorously characterized by the quantum numbers J and M of total angular momentum and its projection. This means that for a level α

with a state vector $|\alpha JM\rangle$ (α represents all other quantum numbers of the state) the standard eigenvalue equations hold:

$$J_z|\alpha JM\rangle = M\hbar|\alpha JM\rangle \quad (9)$$

$$J^2|\alpha JM\rangle = J(J+1)\hbar^2|\alpha JM\rangle \quad (10)$$

In the absence of any preferred direction in space, the levels are all degenerate in M . We will only consider the weak-field case where the magnetic energy ΔE can be obtained using first order perturbation theory. The perturbation V removes the M -degeneracy, though J and M remain good quantum numbers. The energy shift of the state $|\alpha JM\rangle$ is given by:

$$\Delta E = \langle \alpha JM | V | \alpha JM \rangle \quad (11)$$

or

$$\Delta E = B \langle \alpha JM | \mu_z | \alpha JM \rangle. \quad (12)$$

μ_z is the z -component of the vector operator $\boldsymbol{\mu}$. The following operator identity—a special case of the Wigner-Eckhart theorem—is central to our problem. It is valid for states of angular momentum \mathbf{J} for any component K_ν of any vector operator \mathbf{K} .

$$\langle \alpha JM | K_\nu | \alpha JM \rangle = \frac{\langle \alpha JM | J_\nu | \alpha JM \rangle}{\hbar^2 J(J+1)} \langle \alpha JM | \mathbf{J} \cdot \mathbf{K} | \alpha JM \rangle. \quad (13)$$

Applied to the magnetic energy where $K_\nu = \mu_z$ and $\langle \alpha JM | J_z | \alpha JM \rangle = M\hbar$ this gives:

$$\Delta E = -B \frac{M}{\hbar J(J+1)} \langle \alpha JM | \mathbf{J} \cdot \boldsymbol{\mu} | \alpha JM \rangle \quad (14)$$

With $\boldsymbol{\mu}$ given by Eqn. 6 this becomes:

$$\Delta E = \mu_B B M \frac{\langle \alpha JM | J^2 + \mathbf{J} \cdot \mathbf{S} | \alpha JM \rangle}{\hbar^2 J(J+1)} \quad (15)$$

With $\langle \alpha JM | J^2 | \alpha JM \rangle = \hbar^2 J(J+1)$ this gives:

$$\Delta E = \mu_B B M \left(1 + \frac{\langle \alpha JM | \mathbf{J} \cdot \mathbf{S} | \alpha JM \rangle}{\hbar^2 J(J+1)} \right) \quad (16)$$

Thus the magnetic energy is reduced to determining the matrix element of the projection of \mathbf{S} on \mathbf{J} . The matrix element is independent of the choice of the z -axis and will be independent of M . The weak-field Zeeman effect's dependence on M lies entirely in the proportionality expressed in Eqn. 16. The term in parentheses is called the g -factor of the level

$$g_{\alpha J} = 1 + \frac{\langle \alpha JM | \mathbf{J} \cdot \mathbf{S} | \alpha JM \rangle}{\hbar^2 J(J+1)} \quad (17)$$

and Eqn. 16 is then written

$$\Delta E = g_{\alpha J} \mu_B B M \quad (18)$$

1.3 Zeeman Effect in Russell-Saunders Coupled Atoms

For many low- Z atoms, Russell-Saunders (LS) coupling holds reasonably well. For an N -electron atom this means the the state $|\alpha JM\rangle$ is an eigenstate of L^2 , S^2 , and J^2 where $\mathbf{L} = \sum \boldsymbol{\ell}_i$, $\mathbf{S} = \sum \mathbf{s}_i$ and $\mathbf{J} = \mathbf{L} + \mathbf{S}$. In this case, the state $|\alpha JM\rangle$ is often written

$$|\alpha JM\rangle = |\gamma LSJM\rangle. \quad (19)$$

Since $\mathbf{L} = \mathbf{J} - \mathbf{S}$, $L^2 = J^2 + S^2 - 2\mathbf{J} \cdot \mathbf{S}$, from which can be obtained $\mathbf{J} \cdot \mathbf{S} = \frac{1}{2}(J^2 + S^2 - L^2)$. Thus using the eigenvalues of L^2 , S^2 , J^2 , and J_z :

$$\begin{aligned} \langle \gamma LSJM | \mathbf{J} \cdot \mathbf{S} | \gamma LSJM \rangle &= \langle \gamma LSJM | \frac{1}{2}(J^2 + S^2 - L^2) | \gamma LSJM \rangle \quad (20) \\ &= \frac{\hbar^2}{2} (J(J+1) + S(S+1) - L(L+1)) \end{aligned}$$

Substituting this in Eqn. 17 gives

$$g_{\alpha J} = g_{LSJ} = 1 + \frac{J(J+1) + S(S+1) - L(L+1)}{2J(J+1)} \quad (21)$$

g_{LSJ} is called the Landé g -factor and depends only on L , S , and J .

1.4 Zeeman Effect in Neon

Most levels in neon are not well described by LS coupling. Because of this, the g -factor is not given by Eqn. 21.

The dominant configuration of the neon ground state is $1s^2 2s^2 2p^6$ whose only energy level (1S_0) is well described by LS coupling. The next higher configurations are the $1s^2 2s^2 2p^5 3s$ and $1s^2 2s^2 2p^5 3p$ which have, respectively, 4 and 10 energy levels. It turns out that the common 9-electron core $1s^2 2s^2 2p^5$ is reasonably well described as a $2p$ -hole in a closed shell and would, as far as angular momentum is concerned, be similar to a single $2p$ electron, i.e., $\ell_1 = 1$ and $s_1 = 1/2$.

Assuming for the moment that LS coupling holds, then adding a $3s$ electron (as in the lower configuration) with $\ell_2 = 0$ and $s_2 = 1/2$, the normal rules for addition of angular momentum for $\mathbf{L} = \boldsymbol{\ell}_1 + \boldsymbol{\ell}_2$ and $\mathbf{S} = \mathbf{s}_1 + \mathbf{s}_2$ imply that the only allowed value of L would be $L = 1$, (P -states) and that there would be two allowed values for S : $S = 0$ (singlet states) and $S = 1$ (triplet states). Thus, the four states for this configuration would be 1P_1 , $^3P_{0,1,2}$. You should be able to show that the ten states of the second excited configuration in LS coupling would be 1S_0 , 1P_1 , 1D_2 , 3S_1 , $^3P_{0,1,2}$ and $^3D_{1,2,3}$.

As already mentioned, neon is generally not well described in an LS -coupled basis. The states can still be described in this basis, but they will not be pure states. They will be a superposition of such basis states. Because J and M are good quantum numbers, *only basis states of the same J and M will mix*. This limits the number of states in a superposition considerably. Actually, one should include the possibility that there are small admixtures from basis states of the same J and M from other configurations. This is called configuration interaction. This effect is typically small and only states from the same configuration will contribute significantly to a particular level in neon. Thus only the four basis states of the lower configuration could mix, and because two of them—the $^3P_{0,2}$ states—have J -values that appear only once, the $J = 0$ and $J = 2$ levels would be pure and well-described by LS coupling. However, the the two remaining $J = 1$ levels would be superpositions of 1P_1 and 3P_1 basis states.

In the higher configuration, the 3D_3 is the only $J = 3$ state and thus the $J = 3$ level must also be pure and well-described by LS coupling. There will be two $J = 0$ levels each of which will consist of a superposition of 1S_0 and 3P_0 ; there will be four $J = 1$ levels consisting of superpositions of the 1P_1 , 3S_1 , 3P_1 , and 3D_1 , and there will be three $J = 2$ levels consisting of superpositions of 1D_2 , 3P_2 , and 3D_2 .

We might express a particular $|\alpha JM\rangle$ level as follows:

$$|\alpha JM\rangle = \sum_i c_i |\gamma L_i S_i JM\rangle \quad (22)$$

where the c_i are components of the unitary transformation between the states $|\alpha JM\rangle$ and $|\gamma L_i S_i JM\rangle$.

$$c_i = \langle \gamma L_i S_i JM | \alpha JM \rangle \quad (23)$$

If the c_i are known, you should be able to show that the g factor of that level would be given by a weighted sum of Landé g factors:

$$g_{\alpha J} = |c_i|^2 g_{L_i S_i J}. \quad (24)$$

Thus determining the g -factor of a given state has been reduced to finding the coefficients c_i of the level in the LS basis. They depend on the strength of various electron interactions such as spin-orbit and coulomb interactions and can be obtained to a good degree of accuracy from Hartree-Fock calculations. As already mentioned, for many levels in neon, to a reasonable degree, it is found that $j = \ell_1 + s_1$ of the p -hole, 9-electron core is an approximately good quantum number. The possibilities with $\ell_1 = 1$ and $s_1 = 1/2$ are $j = 1/2$ and $j = 3/2$. Thus the core can be ${}^2P_{1/2}$ or ${}^2P_{3/2}$ and one or the other is often given in the designation of a given level. Another approximately good quantum number for neon is found to be $k = j + \ell_2$. For the lower configuration, $\ell_2 = 0$ and thus the only allowed k 's are $k = j$. For the higher configuration, with $\ell_2 = 1$, allowed k -values would be $k = j$, $k = j + 1$, and $k = j - 1$ (if $j \neq 1/2$). Finally, of course, J which is a good quantum number, would—in this scheme of approximately good quantum numbers—be given by $J = k + s_2$ and could therefore take on values of $J = k + 1/2$ and $J = k - 1/2$.

This scheme is called jk coupling and could be described by a state vector

$$|\alpha JM\rangle = |\beta j k JM\rangle. \quad (25)$$

where $\mathbf{j} = \ell_1 + \mathbf{s}_1$, $\mathbf{k} = \mathbf{j} + \ell_2$, $\mathbf{J} = \mathbf{k} + \mathbf{s}_2$. This scheme is illustrated in Table 1, where the wavelengths are given for the transitions between levels of the $1s^2 2s^2 2p^5 3s$ and the $1s^2 2s^2 2p^5 3p$ configurations. The levels according to Paschen notation and some reference values from previous measurements for g -factors are also given.

Paschen	$(^{2S+1}L_J)$	core $n\ell[k]$	\rightarrow		$1s_5$ $(^2P_{3/2})$	$1s_4$ $(^2P_{3/2})$	$1s_3$ $(^2P_{1/2})$	$1s_2$ $(^2P_{1/2})$
	core \downarrow		J	Obs. g	$3s[3/2]$ J=2 1.503	$3s[3/2]$ J=1 1.464	$3s[1/2]$ J=0	$3s[1/2]$ J=1 1.034
$2p_{10}$	$(^2P_{3/2})$	$3p[1/2]$	J=1	1.984	7032	7245	7439	8082
$2p_9$	$(^2P_{3/2})$	$3p[5/2]$	J=3	1.329	6402			
$2p_8$	$(^2P_{3/2})$	$3p[5/2]$	J=2	1.137	6334	6506		7174
$2p_7$	$(^2P_{3/2})$	$3p[3/2]$	J=1	0.669	6217	6383	6533	7024
$2p_6$	$(^2P_{3/2})$	$3p[3/2]$	J=2	1.229	6143	6305		6930
$2p_5$	$(^2P_{1/2})$	$3p[3/2]$	J=1	0.999	5976	6128	6266	6717
$2p_4$	$(^2P_{1/2})$	$3p[3/2]$	J=2	1.301	5945	6096		6678
$2p_3$	$(^2P_{3/2})$	$3p[1/2]$	J=0			6074		6652
$2p_2$	$(^2P_{1/2})$	$3p[1/2]$	J=1	1.340	5882	6030	6164	6599
$2p_1$	$(^2P_{1/2})$	$3p[1/2]$	J=0			5401		5852

Table 1: Wavelength table (in angstroms) for the transitions between the levels of the $1s^22s^22p^53s$ and the $1s^22s^22p^53p$ configurations in neon. Reference g -values are also given.

The basis states of other angular momentum coupling schemes are sometimes approximately eigenstates of other atoms or ions. High Z atoms are sometimes reasonably well described in the jj coupling scheme. For 2-electron atoms and ions, basis states in this scheme are often written $|\tau j_1 j_2 JM\rangle$, where $\mathbf{j}_1 = \boldsymbol{\ell}_1 + \mathbf{s}_1$, $\mathbf{j}_2 = \boldsymbol{\ell}_2 + \mathbf{s}_2$, $\mathbf{J} = \mathbf{j}_1 + \mathbf{j}_2$. The Lk coupling scheme is described by basis states $|\nu LkJM\rangle$, where $\mathbf{L} = \boldsymbol{\ell}_1 + \boldsymbol{\ell}_2$, $\mathbf{k} = \mathbf{L} + \mathbf{s}_1$, and $\mathbf{J} = \mathbf{k} + \mathbf{s}_2$.

There is one other very important set of possible state vectors for a 2-electron atom—the independent electron basis states:

$$|\delta m_{\ell_1} m_{s_1} m_{\ell_2} m_{s_2}\rangle \quad (26)$$

Unlike all the previous state vectors, these states are not eigenstates of J^2 , and thus cannot represent any particular real energy level.

These different sets of state vectors should all be recognized as simply different basis states in which a particular level—eigenstate of the Hamiltonian—can be expressed by a superposition. For some atoms, levels may be nearly pure, i.e., consist of a single basis state, in one or another of these basis sets. However in general, in any basis, many are required. Knowledge of the c_i for a particular level in one basis completely specifies the level, and using angular momentum algebra, one can then find the coefficients in a different basis.

For example, in the lower configuration of neon, there is only one $J = 0$ level. It must therefore be identical equal to the jk -coupled state $(^2P_{1/2})[1/2]0$ (the only $J = 0$ state in this basis) as well as the LS -coupled 3P_0 state (the only $J = 0$ state in this basis). There is also only one $J = 2$ level, which must be pure and equal to both the $(^2P_{3/2})[3/2]2$ basis state or the 3P_2 basis state. These levels, being expressible as pure states in LS -coupling, should have Landé g -factors. Similarly in the higher configuration, there is only one $J = 3$ level which must be identically equal to the $(^2P_{3/2})[5/2]3$ basis state or the 3D_3 state and should have a 3D_3 Landé g -factor.

The g factors of the other states cannot be determined theoretically without knowing their coefficients in some particular basis. Indeed, measured g -factors are used as tests of calculations that provide these coefficients.

While not exactly correct, we may try assuming the states listed in Table 1 are pure jk -coupled states with the quantum numbers as given. Then the coefficients c_i in the LS basis can be obtained from standard angular momentum algebra. Knowing these, the g -factor can be obtained from Eqn. 24.

The most easily understood technique is to express all LS -states and jk -states in a configuration having the same M (but possibly different J 's) as a superposition of the independent particle states (Eqn. 26) of the p -hole and excited electron.

To understand the needed expressions requires the basic formula for addition of angular momenta that expresses the state $|j_3 m_{j_3}\rangle$ of angular momentum $j_3 = j_1 + j_2$ and projection m_{j_3} as a superposition of all possible projection states $|m_{j_1}\rangle$ and $|m_{j_2}\rangle$ of angular momentum j_1 and j_2

$$|j_3 m_{j_3}\rangle = \sum \langle j_1 m_{j_1} j_2 m_{j_2} | j_3 m_{j_3} \rangle |m_{j_1}\rangle |m_{j_2}\rangle \quad (27)$$

where the terms in angle brackets $\langle j_1 m_{j_1} j_2 m_{j_2} | j_3 m_{j_3} \rangle$ are the well known Clebsch-Gordon coefficients, and the sum is over m_{j_1} and m_{j_2} . (See, for example, Messiah, Vol. II, Appendix C.)

Then, for example the $|\gamma LSJM\rangle$ basis state could be obtained as

$$|\gamma LSJM\rangle = \sum \langle \ell_1 m_{\ell_1} \ell_2 m_{\ell_2} | LM_L \rangle \langle s_1 m_{s_1} s_2 m_{s_2} | SM_S \rangle \quad (28)$$

$$\langle LM_L SM_S | JM \rangle |\delta m_{\ell_1} m_{s_1} m_{\ell_2} m_{s_2}\rangle$$

where the sum is over all allowed magnetic quantum numbers except M which would be specified in advance. Note how the C.-G. coefficients show the recoupling of ℓ_1 and ℓ_2 to produce L , s_1 and s_2 to produce S , and L and S to produce J .

A particular $|\alpha j k JM\rangle$ state would be given by:

$$|\alpha j k JM\rangle = \sum \langle \ell_1 m_{\ell_1} s_1 m_{s_1} | j m_j \rangle \langle j m_j \ell_2 m_{\ell_2} | k m_k \rangle \quad (29)$$

$$\langle k m_k s_2 m_{s_2} | JM \rangle |\delta m_{\ell_1} m_{s_1} m_{\ell_2} m_{s_2}\rangle$$

This will not give the transformation coefficients directly but does provide a way to obtain them. This is best illustrated by example. Consider the lower configuration first. Remember we only expect a mixing of the two $J = 1$ states. The technique could be applied to any allowed value of M . $M = 2$ and $M = -2$ can only occur in the $J = 2$ basis states for which we already know the transformation. $M = 0$ can occur for any value of J (four states, in either basis) while $M = 1$ or $M = -1$ can occur for the two $J = 1$ states and the $J = 2$ state in either basis. To keep the number of basis states as small as possible, while including the two $J = 1$ states which are expected to mix, the best choice is to work with the $M = 1$ states.

The independent particle states in the lower configuration where $\ell_1 = 1$, $s_1 = 1/2$ (the core p -hole) and $\ell_2 = 0$, $s_2 = 1/2$ (the $3s$ -electron) (written in the form of Eqn. 26) that can make $M = m_{\ell_1} + m_{s_1} + m_{\ell_2} + m_{s_2} = 1$ are:

$$\begin{aligned} |a\rangle &= |\delta 1\frac{1}{2}0-\frac{1}{2}\rangle \\ |b\rangle &= |\delta 1-\frac{1}{2}0\frac{1}{2}\rangle \\ |c\rangle &= |\delta 0\frac{1}{2}0\frac{1}{2}\rangle \end{aligned} \quad (30)$$

The LS states that have a $M = 1$ component are the 3P_2 , 3P_1 , and 1P_1 . Taking the 3P_1 , for example, there would be three non-zero terms in Eqn. 28, each of which would include one of the independent electron basis states above.

$$\begin{aligned} {}^3P_1(M=1) &= \langle 1100|11\rangle \langle \frac{1}{2}\frac{1}{2}\frac{1}{2}-\frac{1}{2}|10\rangle \langle 1110|11\rangle |\delta 1\frac{1}{2}0-\frac{1}{2}\rangle \\ &+ \langle 1100|11\rangle \langle \frac{1}{2}-\frac{1}{2}\frac{1}{2}\frac{1}{2}|10\rangle \langle 1110|11\rangle |\delta 1-\frac{1}{2}0\frac{1}{2}\rangle \\ &+ \langle 1000|10\rangle \langle \frac{1}{2}\frac{1}{2}\frac{1}{2}\frac{1}{2}|11\rangle \langle 1011|11\rangle |\delta 0\frac{1}{2}0\frac{1}{2}\rangle \\ &= \frac{1}{2}|a\rangle + \frac{1}{2}|b\rangle - \sqrt{\frac{1}{2}}|c\rangle \end{aligned} \quad (31)$$

The full transformation could be written in matrix form:

$$\begin{pmatrix} {}^3P_2 \\ {}^3P_1 \\ {}^1P_1 \end{pmatrix} (M=1) = \begin{pmatrix} \frac{1}{2} & \frac{1}{2} & \sqrt{\frac{1}{2}} \\ \frac{1}{2} & \frac{1}{2} & -\sqrt{\frac{1}{2}} \\ \sqrt{\frac{1}{2}} & -\sqrt{\frac{1}{2}} & 0 \end{pmatrix} \begin{pmatrix} |a\rangle \\ |b\rangle \\ |c\rangle \end{pmatrix} \quad (32)$$

Again in the lower configuration, the jk states that have a $M = 1$ component are the $({}^2P_{3/2})[3/2]2$, $({}^2P_{3/2})[3/2]1$, and $({}^2P_{1/2})[1/2]1$. Taking the $({}^2P_{3/2})[3/2]1$, for example, there would be three non-zero terms for its $M = 1$ component in Eqn. 29.

$$\begin{aligned} ({}^2P_{3/2})[3/2]1(M=1) &= \langle 11\frac{1}{2}\frac{1}{2}|\frac{3}{2}\frac{3}{2}\rangle \langle \frac{3}{2}\frac{3}{2}00|\frac{3}{2}\frac{3}{2}\rangle \langle \frac{3}{2}\frac{3}{2}\frac{1}{2}-\frac{1}{2}|11\rangle |\delta 1\frac{1}{2}0-\frac{1}{2}\rangle \\ &+ \langle 11\frac{1}{2}-\frac{1}{2}|\frac{3}{2}\frac{3}{2}\rangle \langle \frac{3}{2}\frac{1}{2}00|\frac{3}{2}\frac{3}{2}\rangle \langle \frac{3}{2}\frac{1}{2}\frac{1}{2}\frac{1}{2}|11\rangle |\delta 1-\frac{1}{2}0\frac{1}{2}\rangle \\ &+ \langle 10\frac{1}{2}\frac{1}{2}|\frac{3}{2}\frac{3}{2}\rangle \langle \frac{3}{2}\frac{1}{2}00|\frac{3}{2}\frac{3}{2}\rangle \langle \frac{3}{2}\frac{1}{2}\frac{1}{2}\frac{1}{2}|11\rangle |\delta 0\frac{1}{2}0\frac{1}{2}\rangle \\ &= \sqrt{\frac{3}{4}}|a\rangle - \sqrt{\frac{1}{12}}|b\rangle - \sqrt{\frac{1}{6}}|c\rangle \end{aligned} \quad (33)$$

The full transformation could be written in matrix form:

$$\begin{pmatrix} ({}^2P_{3/2})[3/2]2 \\ ({}^2P_{3/2})[3/2]1 \\ ({}^2P_{1/2})[1/2]1 \end{pmatrix} (M = 1) = \begin{pmatrix} \frac{1}{2} & \frac{1}{2} & \sqrt{\frac{1}{2}} \\ \sqrt{\frac{3}{4}} & -\sqrt{\frac{1}{12}} & -\sqrt{\frac{1}{6}} \\ 0 & \sqrt{\frac{2}{3}} & -\sqrt{\frac{1}{3}} \end{pmatrix} \begin{pmatrix} |a\rangle \\ |b\rangle \\ |c\rangle \end{pmatrix} \quad (34)$$

Using matrix inversion and multiplication we can get the jk basis states as a superposition of the LS basis states:

$$\begin{pmatrix} ({}^2P_{3/2})[3/2]2 \\ ({}^2P_{3/2})[3/2]1 \\ ({}^2P_{1/2})[1/2]1 \end{pmatrix} = \begin{pmatrix} 1 & 0 & 0 \\ 0 & \sqrt{\frac{1}{3}} & \sqrt{\frac{2}{3}} \\ 0 & \sqrt{\frac{2}{3}} & -\sqrt{\frac{1}{3}} \end{pmatrix} \begin{pmatrix} {}^3P_2 \\ {}^3P_1 \\ {}^1P_1 \end{pmatrix} \quad (35)$$

Note that this transformation is actually independent of M even though it was derived from $M = 1$ basis states. Note also the expected result that the $({}^2P_{3/2})[3/2]2$ is a pure 3P_2 state. Having the c_i for the jk states now allows us to determine the g -factors in this basis. From Eqn. 21 we have $g({}^3P_1) = 3/2$ and $g({}^1P_1) = 1$. Thus $g(({}^2P_{3/2})[3/2]1) = (1/3)(3/2) + (2/3)(1) = 7/6 = 1.167$ and $g(({}^2P_{1/2})[3/2]1) = (2/3)(3/2) + (1/3)(1) = 4/3 = 1.333$.

Before finishing up, let's explore an easier method to obtain the g -factor of a level when the level's coefficients are determined in the independent electron basis. This is actually quite simple because the perturbation $V = (B\mu_B/\hbar)(L_z + 2S_z)$ is diagonal in this basis.

$$\langle \delta m_{\ell_1} m_{s_1} m_{\ell_2} m_{s_2} | V | m_{\ell_1} m_{s_1} m_{\ell_2} m_{s_2} \rangle = B\mu_B [m_{\ell_1} + m_{\ell_2} + 2(m_{s_1} + m_{s_2})] \quad (36)$$

Thus for the basis states $|a\rangle$, $|b\rangle$, and $|c\rangle$ we get

$$\begin{aligned} \langle a | V | a \rangle &= B\mu_B \cdot 1 \\ \langle b | V | b \rangle &= B\mu_B \cdot 1 \\ \langle c | V | c \rangle &= B\mu_B \cdot 2 \end{aligned} \quad (37)$$

From which you should be able to show that, for example, for the 3P_1 ($M = 1$) given by Eqn. 31,

$$\begin{aligned} \Delta E &= B\mu_B \left(\frac{1}{4} \cdot 1 + \frac{1}{4} \cdot 1 + \frac{1}{2} \cdot 2 \right) \\ &= \frac{3}{2} B\mu_B, \end{aligned} \quad (38)$$

and for the $(^2P_{3/2})[3/2]1$ ($M = 1$) given by Eqn. 33,

$$\begin{aligned}\Delta E &= B\mu_B \left(\frac{3}{4} \cdot 1 + \frac{1}{12} \cdot 1 + \frac{1}{6} \cdot 2 \right) \\ &= \frac{7}{6} B\mu_B.\end{aligned}\tag{39}$$

Comparing with Eqn. 18 gives, as obtained previously, $g(^3P_1) = 3/2$ and $g(^2P_{3/2})[3/2]1 = 7/6$

Finally, note that the g -factors of the levels labeled $(^2P_{1/2})[1/2]1$ and $(^2P_{3/2})[3/2]1$ in the table are 1.034 and 1.464, respectively: much closer to the values expected for the LS -coupled 1P_1 and 3P_1 states, indicating these states are more nearly pure in the LS -basis. It is interesting to note however that for the higher- Z inert gases such as Kr and Xe the g -factors do begin to come close to the jk -coupled state values of 1.167 and 1.333.

2 Experiment

2.1 Setup

The apparatus is shown in Fig. 1. Make sure you understand the theory of the Fabry-Perot interferometer. The optical setup marginally requires that the collimating lens has the neon discharge lamp at its focus so that all light from a given point on the source goes through the Fabry-Perot FP at a single angle. The focussing lens must then have the entrance slit at its focus to image the source and FP ring pattern on the entrance slit. (Use the 1 or 2 mm entrance slit on the brass slit plate.) When this is not done properly, the telescope when focussed on the slit image, (which is now dispersed by the grating and formed at the exit focus plane) will not show clear interference rings. The rings can still be made to come into focus, but at the expense of losing the sharp slit images. If the ring pattern does not show the lowest order ring near the center of the slit image, it means the FP is not perpendicular to the beam and its overall orientation should be adjusted.

To align the optical flats on the FP, view the source through the FP by eye. You should see rings superimposed on the source. If, as you move your eye perpendicular to the beam direction and parallel to a line from the center of the FP to one of the adjustment screws, the rings move in or out, that screw must be adjusted.

The magnetic field is adjusted with the dial on the current regulator. It's indicator should always remain in the range from 3-7 mAmp, and especially should never be allowed to remain at high values. The power supply variac dial must be turned up and down together with the current regulator to keep the regulator in its working range. The indicator on the power supply gives a rough value for the magnet current and should never be allowed to go above 5 Amps or the magnetic forces may pull the pole pieces together and break the yoke in which they are mounted.

When necessary, the field strength should be measured with a Hall probe. The probe face must be oriented parallel to the pole faces and the Hall voltage should be measured twice at the same Hall current with the probe turned 180° between measurements. The voltage should change sign. The average voltage magnitude should be used in calculating the field strength.

The discharge tends to be more difficult to keep on at high field strengths and this problem can depend on the age of the tube so try several tubes and turn up the tube voltage if needed to keep the discharge on. Can you see any shift in the ring pattern as you do this? Don't leave on the high voltage when it is unnecessary as this shortens the tube life.

2.2 Measurements

You will use the FP in a way different from that suggested in Melissinos. A single frequency source produces a single set of rings when the FP is interposed. As the frequency increases or decreases the rings move in or out. The frequency change needed to move the pattern one ring (so that a ring moves to where the ring just inside it or outside it was originally) is called the free spectral range ν_f of the FP ($\nu_f = c/2l$) where c is the speed of light and l is the separation between the optical flats (9.995 mm for our FP).

According to the theory, in a magnetic field, a state of a given J splits into $2J + 1$ components; the change in energy given by Eqn. 18. When you look at the spectrum through the telescope, you will see the visible spectrum of neon, part of which is diagrammed in Fig. 2. Because the Zeeman splittings are small, the wavelength shifts in the magnetic field are much too small to resolve with the spectrograph. Nonetheless, within any particular spectral line, depending on the J of the initial and final levels, in a magnetic field there are several transitions of slightly different energies being observed, which change as the B -field is turned up.

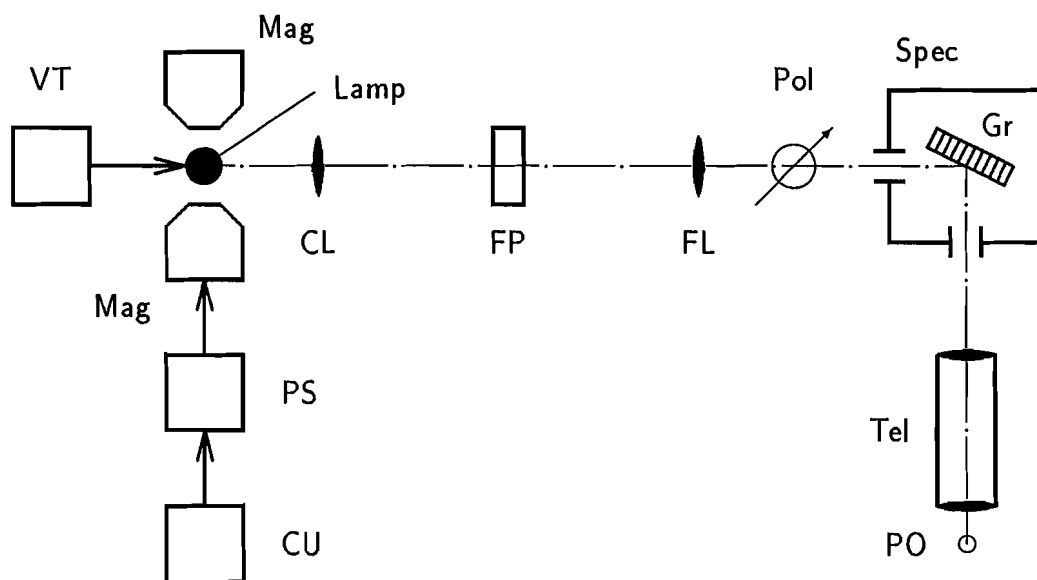


Figure 1: Overview of the experimental setup with the following main components: Neon discharge lamp (Lamp) with variable transformer (VT), high field magnet (Mag) with power supply (PS) and control unit (CU), a collimating lens (CL), the FABRY – PEROT interferometer (FP), a focusing lens (FL), a polarizer (Pol), a spectrograph (Spec) with reflection grating (Gr), and a telescope (Tel). Zeeman splittings can be observed at the point of observation (PO).

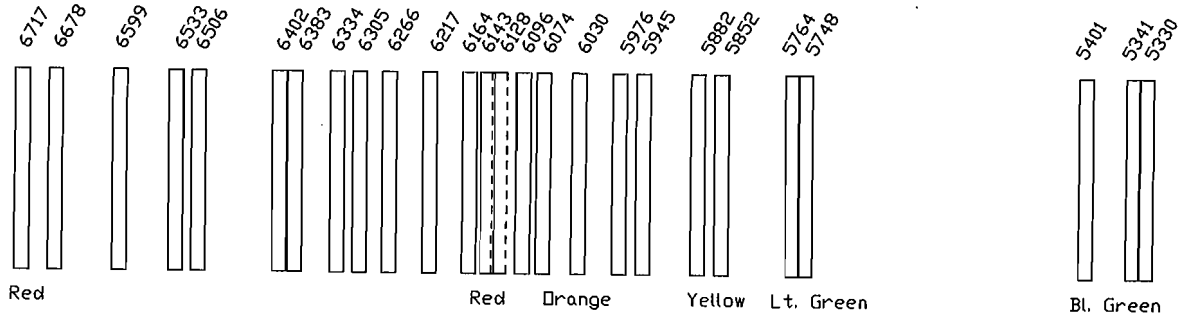


Figure 2: The spectrum (inverted as viewed through a telescope) of neon. Some weaker lines are not shown.

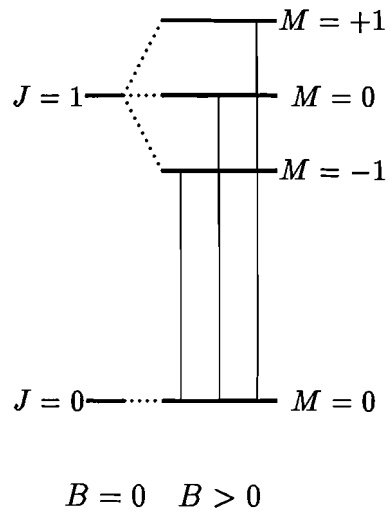


Figure 3: Zeeman effect in the case of a $J = 0 \rightarrow J = 1$ transition. The energy splitting between adjacent sublevels in the $J = 1$ level is $g\mu_B B$.

This is most easily demonstrated for a $J = 1$ to 0 transitions as in Fig. 3. In this case, there is a single frequency when there is no field. Thus when the line is viewed with the FP interposed, there should be a single set of rings. When the field is then turned on and slowly increased, two components will change in frequency at the same rate—one will increase and the other will decrease, while a third component does not change frequency. This would be observed as two new rings splitting off each of the original rings: one moving inward and one moving outward, while the original rings remains stationary.

As the field is further increased, the rings moving outward will meet the rings moving inward halfway between the stationary rings. This is easily observed as the two rings meet and the ring pattern becomes twice as dense as the original with all rings uniformly spaced. This (double density) pattern distinguishes the point at which the frequency shift $\Delta\nu = \Delta E/h = g\mu_B B/h$ of each component has shifted by $\nu_f/2$. Then, a measurement of the B -field strength will allow for a determination of the g -factor.

Continuing to increase the field will cause the rings to move until they next meet up with the stationary rings. This will be obvious as the three rings merge into a single ring (single density). At this point you know that the frequency shift $\Delta\nu = g\mu_B B/h = \nu_f$, and a measurement of the B -field strength at this point will allow for a determination of the g -factor.

In fact, any time you can distinguish from a particular pattern that the frequency shift, expressed as a fraction of ν_f , i.e., $\Delta\nu = n\nu_f$, has some particular value of n , such as $n = 1/2$ and $n = 1$ above, you expect that

$$n = \frac{g\mu_B}{h\nu_f} \cdot B \quad (40)$$

The measurements are somewhat better when a polarizer is used to cut down the number of frequency components observed through the FP. Recall that the dipole selection rules require $\Delta M = 0, \pm 1$. The polarization of the light from different values of ΔM depends on the direction of light propagation relative to the field direction. See Fig. 4. The radiation from the $\Delta M = \pm 1$ transitions can be viewed classically as arising from a charge (the electron) in a circular orbit rotating in either a clockwise or counterclockwise direction with the field direction along the axis of rotation. The $\Delta M = 0$ transitions arise from a charge oscillating back and forth along the field direction.

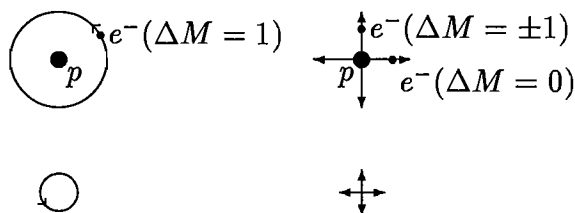


Figure 4: Classical picture of the electronic motion (top) and emitted radiation (bottom) viewed from two directions relative to the magnetic field: B is out of the page (left) and towards the right (right).

On the left in the figure, the field points out of the page. (Only the $\Delta M = 1$ clockwise electronic rotation is shown. The $\Delta M = 0$ oscillation along the field direction is head-on and also not shown.) Below this figure, the radiation observed coming out of the page is shown. Viewed from this direction only left circular and right circular (shown) polarized light is observed. No radiation from the $\Delta M = 0$ is emitted in this direction, as the oscillations are along the observation direction.

On the right in this figure is the relative orientations used in this experiment. When the same charge oscillations are viewed from a point out of the page with the field pointing towards the right, (left view of the figure on the left) the $\Delta M = 0$ oscillations are now horizontal. The $\Delta M = \pm 1$ rotations, in this view, appear as oscillations along a vertical line. Viewed, once again, coming out of the page, the radiation (below) from the $\Delta M = 0$ transitions is linearly polarized along the field direction and from the $\Delta M = \pm 1$ transitions it is linearly polarized perpendicular to the field direction.

If a polarizer is used and oriented to pass the two $\Delta M = \pm 1$ shifting frequencies and block the $\Delta M = 0$ component, then at a field strength such that $\Delta\nu = \nu_f/2$ the inward and outward moving rings meet, but the original ring would be absent. Thus there would be just as many rings as there are without any field (single density), but each ring would be shifted half a position over. Before this occurs, when $\Delta\nu = \nu_f/4$, the rings will have all moved in or out $1/4$ of a ring spacing, and the pattern will have twice as many rings as the $B = 0$ pattern (double density) and they will be uniformly spaced. Both these patterns are easily distinguished. The double density

ring pattern repeats at $n = \Delta\nu/\nu_f = 1/4, 3/4, 5/4$, etc., and the single density pattern at $n = \Delta\nu/\nu_f = 1/2, 1, 3/2$, etc. Depending on the g -factor you should be able to see shifts of $1/4, 1/2, 3/4, 1$, and maybe $5/4$ of ν_f , for most of the $J = 0$ to $J = 1$ and $J = 1$ to $J = 0$ transitions.

You may want to look at the $\Delta M = 0$ transitions (by turning the orientation of the polarizer) of the $J = 2$ to $J = 1$ transitions. Think about what the rings should do, what ring patterns can be observed to give useful information about the frequency shifts, and what information is obtained. Hint: well defined patterns occur at $\Delta\nu/\nu_f = 1/3, 2/3, 4/3$, etc., (triple density patterns), $\Delta\nu/\nu_f = 1/2, 3/2$, etc., (double density patterns), and $\Delta\nu/\nu_f = 1, 2, 3$, etc., (single density patterns). The information obtained will be about the difference between the g 's of the two levels.

2.3 Analysis

For each transition studied, make a table of $n = \Delta\nu/\nu_f$, the Hall probe current and voltage (two readings, with the probe oriented in both directions), and B calculated in Tesla from the Hall probe readings. Make plots of $n = \Delta\nu/\nu_f$ versus B . Put error bars on the B values. Perform a linear regression (with zero intercept, as predicted by theory) and obtain the g -factors (or Δg for a $J = 2$ to $J = 1$ transition) from the slope m . From the model (Eqn. 40) $m = g\mu_B/h\nu_f$.

Make a table including the wavelengths, the two states involved in the transition, the slope, and measured g -factors (or Δg) with uncertainties and compare them with the previously measured values.

3 Questions

1. How well can you observe particular patterns? To determine the uncertainty in B , vary the strength of B within a range over which the pattern is not distinguishably changing. Is one particular pattern more distinguishable (have a smaller range in B) than another?
2. Derive Eqn. 24 from Eqn. 22.
3. Find the inverse matrix and perform the matrix multiplication to derive Eqn. 35.

4. The g -sum rule, derivable from Eqn. 24 and the fact that the c_i are elements of a unitary transformation, states that sum of the g -factors over a particular J of a configuration should be equal to the sum of the g -factors for all possible LS -basis states in that configuration of that same J . Check the g -sum rule by computing the sum of reference g -values of the two $J = 1$ transitions in the lower configuration and comparing that sum with the sum of the Landé g -factors for the 1P_1 and 3P_1 states. Repeat this procedure for both the sum over the $J = 1$ and over the $J = 2$ levels in the higher configuration. Show all work.
5. Show that for a transition between a $J = 2$ and $J = 1$ level, with the polarizer oriented to pass light polarized along the field direction, the frequencies expected to be observed are ν_0 , and $\nu_0 \pm (g_2 - g_1)\mu_B B/h$. where ν_0 is the frequency of the line in zero field, and g_2 and g_1 are the g -factors of the two levels involved. Draw a figure showing the sublevel splittings in both levels, assuming $g_1 \neq g_2$, and draw lines between the levels showing the transitions that will be observed.

4 References

E.U. Condon and G.H. Shortley, **The Theory of Atomic Spectra**, (Cambridge University Press, 1970).

J.C. Slater, **Quantum Theory of Atomic Structure**, (McGraw-Hill, New York, 1960).

A. Messiah, **Quantum Mechanics**, (Wiley, New York).

A.C. Melissinos, **Experiments in Modern Physics**, (Academic Press, New York, 1966).